Synchrotron Radiation Effects in the IR Solenoid Flux Excluder

Peter Tenenbaum
LCC-Note-0007
Draft 23-September-1998

Abstract

We examine the emittance dilution due to synchrotron radiation in the fringing fields at the end of the "flux excluder" solenoid which protects the final doublet quadrupoles from the main detector solenoid field, and also the effect of SR in the main solenoid field itself. Because the deflection due to the excluder fringe field is opposite in polarity from that of the main solenoid, the resulting dispersive rays cancel at the IP; as a result the synchrotron radiation from the two magnetic fields produces only a small dilution of the vertical spot size. The contribution to the spot size from the finite opening angle of the synchrotron flux is found to be comparable to the contribution from solenoidal dispersion, and both are acceptable. We conclude that SR considerations do not rule out use of a flux excluder, and that the range of crossing angles and solenoidal fields available is large.

1 introduction

One of the more controversial aspects of the NLC IR design is the configuration of the detector solenoid and the corresponding flux exclusion solenoids: the main detector solenoid produces a large field (presently expected to be 4 Tesla) in the entire volume of the IR, while a pair of smaller solenoids with the same number of windings per centimeter, powered in parallel with the main solenoid but in opposite polarity, cancel the resulting B_z in the area surrounding the final magnets. The purpose of the flux excluder is to have a zero-field region around the permanent magnets and to prevent depolarization effects in the crucial last lenses of the collider. Figure 1 shows a cartoon of the layout of the system.

The main solenoid and the flux excluders are all aligned with their axes along the IP axis, as shown in Figure 1, while the beam emerges from the flux excluder with an angle relative to the solenoidal field (presently assumed to be 10 mrad). Consequently the beam passes off-center through the fringe field of the flux excluder, potentially exposing the beam to a strong transverse field next to the detector.

In this Note we study only the synchrotron radiation effects of the flux excluder/solenoid system. A further study of optical effects, while worthwhile, has not been done at this time.

2 Magnetic field of a Solenoid

The magnetic field of a long solenoid of radius R can be expressed by integration of the law of Biot and Savart [1]:

$$d\mathbf{B} = \frac{\mu_0 I}{4\pi}\frac{d\mathbf{l}\times\mathbf{r}}{r^3}. \tag{1}$$

Consider the situation pictured in Figure 2: the point of interest is located at (x_0, z_0) from the origin of coordinates, while the field is contributed by an annulus of charge, thickness dz and radius R, a distance z' from the origin of coordinates. A point on the annulus at azimuthal angle θ has a vector $d\mathbf{l}$ given by:

$$d\mathbf{l}(\theta) = Rd\theta\left(\hat{y}\cos\theta - \hat{x}\sin\theta\right), \tag{2}$$

and a vector to the point of interest given by:

$$\mathbf{r} = \hat{z}(z_0 - z') + \hat{x}(x_0 - R\cos\theta) - \hat{y}(R\sin\theta). \tag{3}$$

We may replace I with Jdz, where J is the current density; in order to achieve a solenoidal field of B_0, we find that $\mu_0 J = B_0$, and thus may write:

$$d\mathbf{B} = \frac{B_0}{4\pi}Rdzd\theta\frac{\hat{z}(R - x_0\cos\theta) + \hat{x}(z_0 - z')\cos\theta + \hat{y}(z_0 - z')\sin\theta}{\left[(z_0 - z')^2 + x_0^2 + R^2 - 2x_0R\cos\theta\right]^{3/2}}. \tag{4}$$

To obtain the magnetic field at any point, it remains only to integrate Equation 4 about a full circle and from $-\infty$ to zero in z'.

The B_y term in Equation 4 can readily be evaluated and, as required by symmetry, is identically zero. The other two terms are sufficiently daunting that numerical integration (via Matlab) was used. For a flux excluder with 10 cm radius extending to 1.5 meters from the IP embedded in a 40 kG main solenoid, and a 10 mrad crossing angle, Figure 3 shows the fields experienced by the beam as a function of z. The top and middle plots show the magnetic fields, B_r and B_z, in the IP coordinate system; the bottom plot shows $B_{transverse}$, the field which is transverse to the electron beam, obtained by rotating the top two plots through 10 mrad in x.

An important feature of Figure 3 is that the field components perpendicular to the beam direction from the fringe field of the flux excluder and from the main solenoidal field are opposite in direction, as shown in Figure 4. Consequently the peak field experienced by the beam is 1.3 kG over several centimeters around the exit of the flux excluder. This will have important consequences which are discussed in the next section.

3 Synchrotron Radiation Growth

The relevant equation for the IP region is not the one governing emittance growth but an equation which exclusively evaluates the growth of the beam size at the IP. Following Irwin [2],

$$\Delta\sigma_y^2 = c_u r_e \bar{\lambda}_e \gamma^5 \int ds R_{36}^2(s) \left|\frac{1}{\rho(s)}\right|^3, \tag{5}$$

where r_e and $\bar{\lambda}_e$ are the classical electron radius and the electron Compton wavelength, respectively (2.8×10^{-15} m and 3.9×10^{-13} m, resp.), c_u is a synchrotron radiation constant with value approximately 1.32 [3], and γ is the relativistic factor of the beam. The R_{36} term is the R_{36} from the field point to the IP; this can also be expressed in terms of the dispersion at the IP: $R_{36}(s) = \eta_y^* - \eta_y(s)$, assuming that η_y is zero at the entrance of our system..

The dispersion at all points in the system can be derived from the fact that the second derivative of the dispersion, η'', is equal to $B(z)/B\rho$. For a perfect solenoid, Irwin found that Equation 5 can be reduced to a simple expression:

$$\Delta\sigma_y^2 = \frac{c_u r_e \bar{\lambda}_e}{20} \left(\frac{B_0 \theta_{\rm cross} L^* \gamma}{2B\rho}\right)^5. \tag{6}$$

For the present NLC parameters (B_0 = 40 kG, $\theta_{\rm cross}$ = 20 mrad, L^* = 2 meters), the contribution in quadrature with the IP spot is 0.13 nm.

In the more complex magnetic field pictured in Figure 3, and in the absence of focusing elements, we can obtain η' by numerically integrating $B(z)/B\rho$, and η' can be integrated again to obtain η as a function of z. Figure 5 shows the resulting η' and η functions, assuming no correction at the IP. Note that the dispersion at the IP is naturally nearly zero (actually it is about 400 nanometers), due to the change in sign of the bending field.

With $\eta(z)$ and $B(z)$ in hand, we may now, finally, numerically integrate to determine the SR contribution to spot size dilution throughout the flux excluder region. Figure 6 shows the individual contributions to σ_y^2 (in square nanometers) from each point along the beam's path. Because the dispersion is zero at the entrance of the system and nearly zero at the exit, the R_{36} elements are small everywhere, leading to a total contribution to the beam size of 26 picometers added in quadrature.

While the IP dispersion is small, it is not yet small enough to avoid serious luminosity dilution (for a 0.3% energy spread, 400 nm of dispersion contributes 1.2 nm to the IP spot size). Fortunately the needed correction is small: for this study, a 40 cm steering magnet with a bending field of 10 gauss was used (although one could also move the final lens if desired). Figure 7 shows the resulting η and η' functions. As expected the dispersion functions are nearly identical with those in Figure 5.

Figure 8 shows the contributions to $\Delta\sigma_y^2$ in the corrected case. In this case, 25 picometers are added in quadrature to the beam size.

4 Properties of the Synchrotron Radiation

To quantify the synchrotron emissions in these cases, we can use equations in convenient units supplied by Roy [4]. The critical energy in MeV is given by:

$$u_c = 2.96 \times 10^{-13} \frac{\gamma^3}{\rho} \tag{7}$$

and the number of photons emitted per second is given by:

$$N = 3.1617 \times 10^6 \frac{\gamma}{\rho}, \tag{8}$$

where ρ is specified in meters. For a 500 GeV beam at the speed of light passing through a 40 cm of flux excluder with a field of 1.3 kG, the critical energy is 22 MeV and 0.32 photons are emitted per electron. The characteristic transverse momenta of the photons, given by u_c/γ, is 22 eV. For a 500 GeV beam, this provides a kick of 14 picoradians. Over 1.5 meters, the resulting increase in beam size is roughly 21 picometers. This is comparable to the traditional synchrotron radiation effect computed above, and both terms appear negligible. While the effects of the 40 cm steering magnet are not included here, we can assume that the energy loss and transverse kick due to the 10 gauss field is truly miniscule.

As the beam is steered first up and then down (or vice-versa) in the IR solenoidal fields, a vertical synchrotron radiation fan is emitted from +12 microradians to -18 microradians relative to the axis of the solenoids and the detector. Appropriate masking or channels for removal of the light are required.

5 Scaling Laws

The synchrotron radiation dilution due to a simple solenoid with crossing angle at the IP was found to scale as $(B_0\theta_{\rm cross})^5$, and to be independent of energy. The dilution due to the flux excluder and the corrector magnet also scales as $B_0^5\theta_{\rm cross}^5$, and is also independent of energy. The transverse deflection due to the opening angle of the synchrotron radiation goes as u_cN/γ, which can be reduced to $\gamma(B_0\theta)^2$. Increasing either the crossing angle or the solenoidal field by 50% is acceptable from a beam size point of view, but doubling either one would add 0.8 nm in quadrature with the beam size. This is probably unacceptable. The opening-angle effect remains miniscule even if the bending field or the crossing angle is doubled.

The fringe field of the flux excluder seen by the beam is roughly inversely proportional to the radius of the flux excluder, and can also be reduced by extending the flux excluder further into the detector: as the beams approach the IP, the offset from the axis of the solenoids is reduced. In principle the length and diameter of the flux excluder can be tuned to provide a field which exactly cancels the IP dispersion, but in practice this probably implies construction and installation tolerances which are hard to meet, and a tuning corrector remains desirable.

6 Conclusions

For the "canonical" NLC IR parameters, the beam size dilution from the flux excluder fringe field and the main detector solenoid is 2% of the nominal beam size added in quadrature; the total contribution is therefore negligible. The dilution remains acceptable if either the angle or the field is increased by 50%, but is unacceptable if either one is doubled.

One beneficial effect of the flux excluder fringe field is that it tends to cancel the dispersion introduced by the main solenoid; it is this effect which causes the SR dilution to be small. If the NLC IR is built without a flux excluder, it will be necessary to build a dipole deflector to perform the same function, and at the same location. Consequently, the presence or absence of a flux excluder has no effect on the SR dilution at the IP, since if the flux excluder was not there we would build another magnet which would have the same effect.

7 Unresolved Optics Issues

The optical effects of the flux excluder's fringe field, and corrections for same, have not been considered. Also, there are several consequences of the deflection of the beams in the solenoid which still need to be examined. The most serious of these is that the beams are deflected vertically by a large amount by the time they reach the opposite flux excluder: this means that (relative to the case with solenoid and flux excluder off), the beams now have a large offset and angle entering the extraction line, and these should probably be taken out by steering magnets in the extraction side of the flux excluder. Also, the flux excluder now kicks the beam both horizontaly and vertically, since the fringe field is purely radial and the beam now has both horizontal and vertical offsets.

8 Acknowledgements

The authors would like to thank T. Raubenheimer for guidance and insight into the relevant issues.

References

[1] D. Halliday and R. Resnick, *Physics*, 3rd Ed. (New York: Wiley, 1978) 759.

[2] The NLC Design Group, *Zeroth Order Design Report for the Next Linear Collider* (Stanford: SLAC, 1996) 773.

[3] M. Sands, "The Physics of Electron Storage Rings", SLAC-121 (Stanford: SLAC, 1970) 118.

[4] G. Roy, "A New Method for the Simulation of Synchrotron Radiation in Particle Tracking Codes," Nucl. Inst. Meth. **A298** 128-133 (1990).

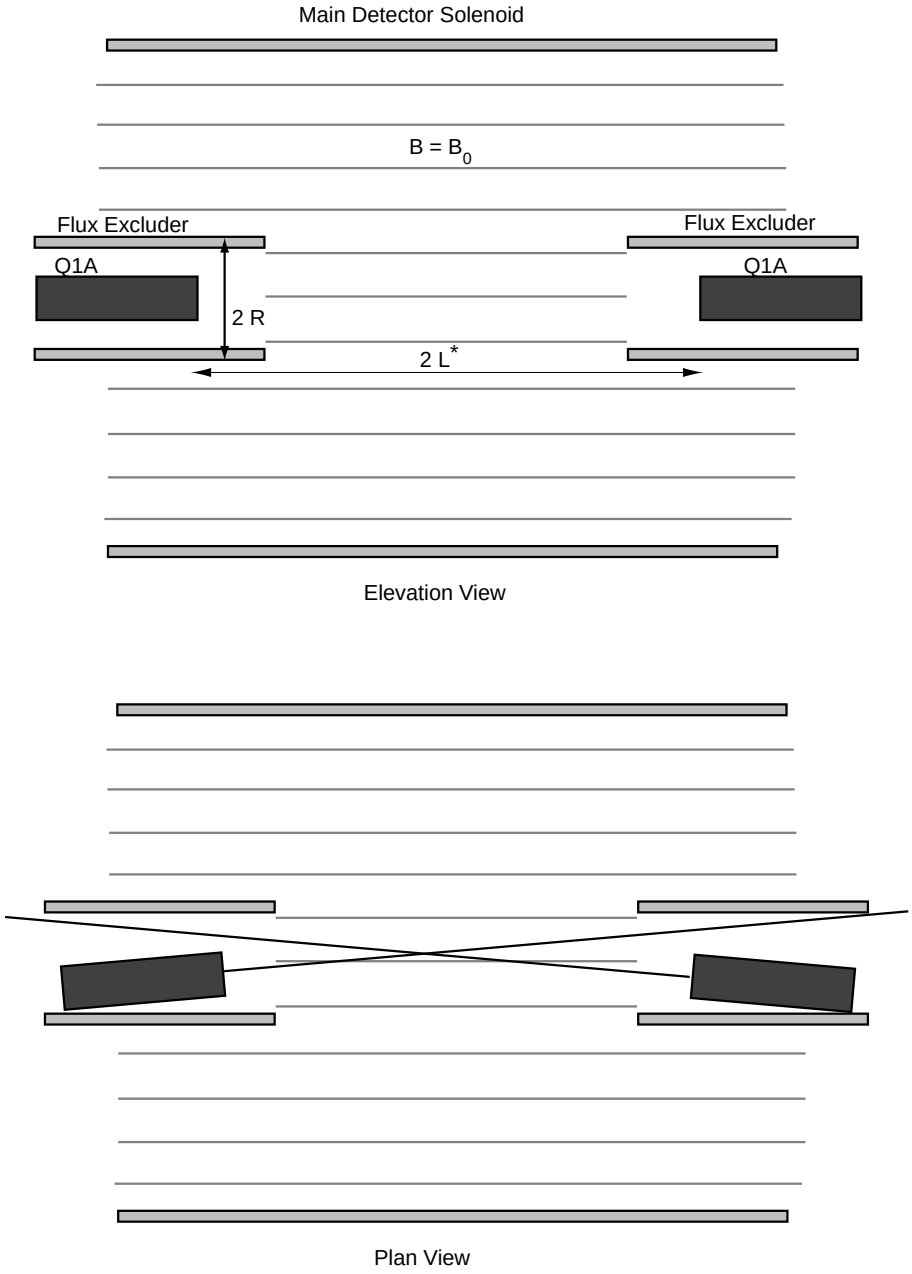

Figure 1: Diagram of the IR, with final quads embedded in the flux excluders, which are in turn embedded in the main detector solenoid. The flux excluder is assumed to extend some distance past the last quad (50 centimeters used in the text).

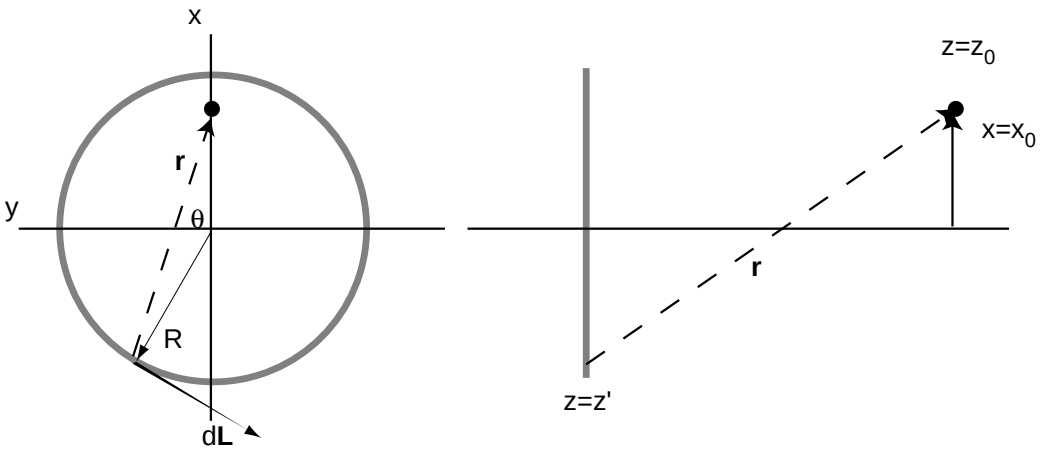

Figure 2: Diagram of a single winding of a solenoid, showing the dimensions necessary to compute the magnetic field via the Biot-Savart law.

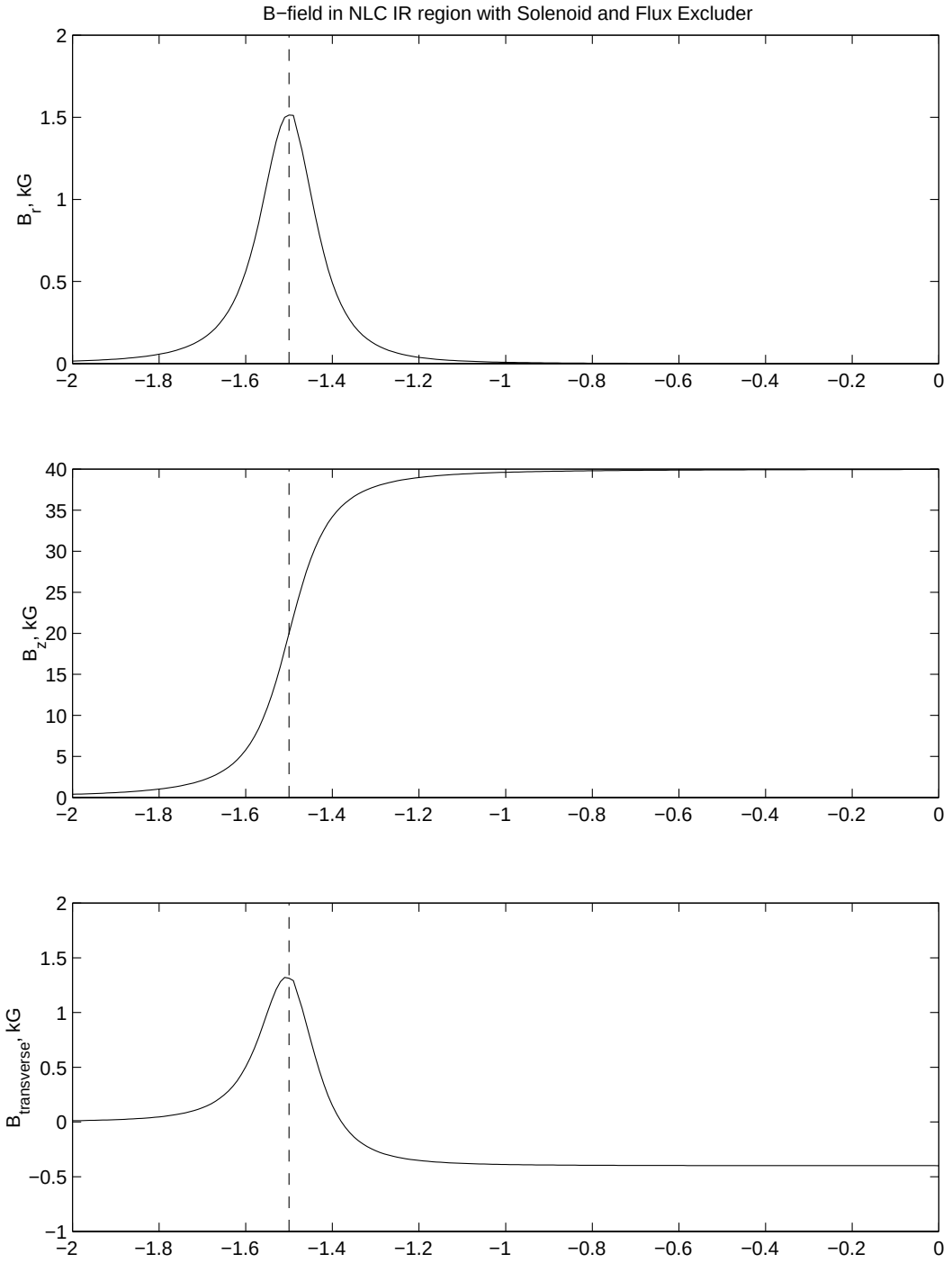

Figure 3: Magnetic field experienced by the beam passing off-axis through the flux excluder and detector solenoids. The longitudinal and radial fields are shown, as well as the actual field perpendicular to the beam. The dashed line is the edge of the flux excluder.

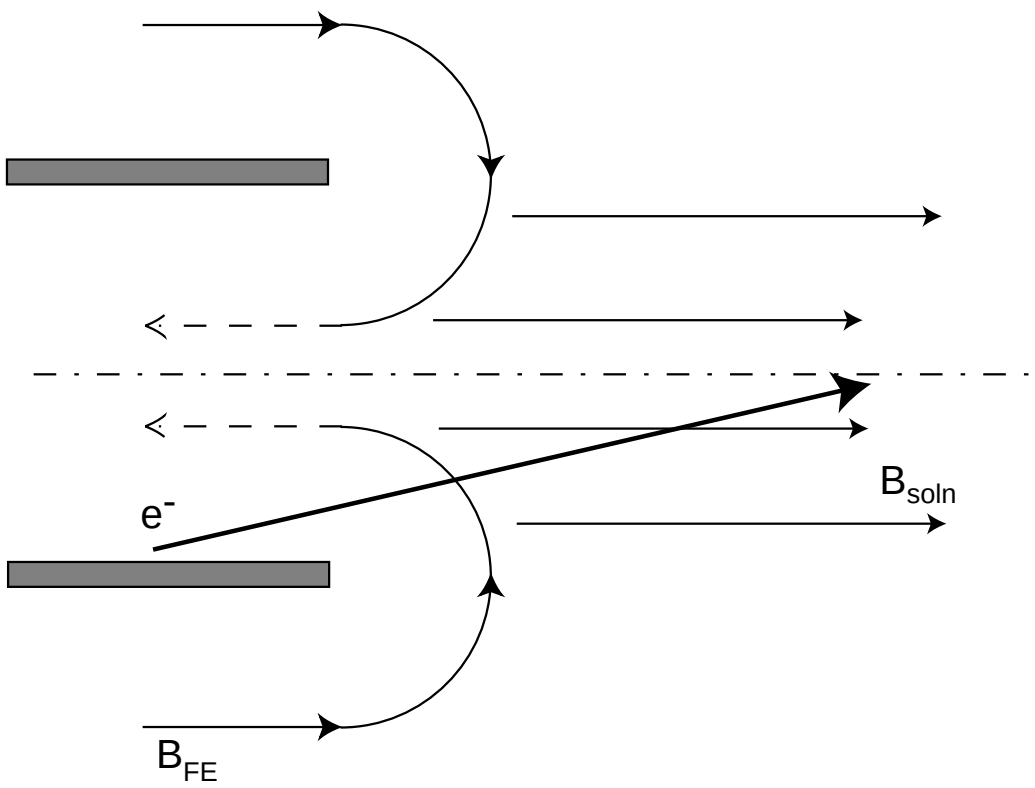

Figure 4: Close-up view of the beam exiting the flux excluder and entering the main solenoid field. The transverse field due to the flux excluder fringe is opposite in direction to the transverse field from passing through the main solenoidal field at an angle.

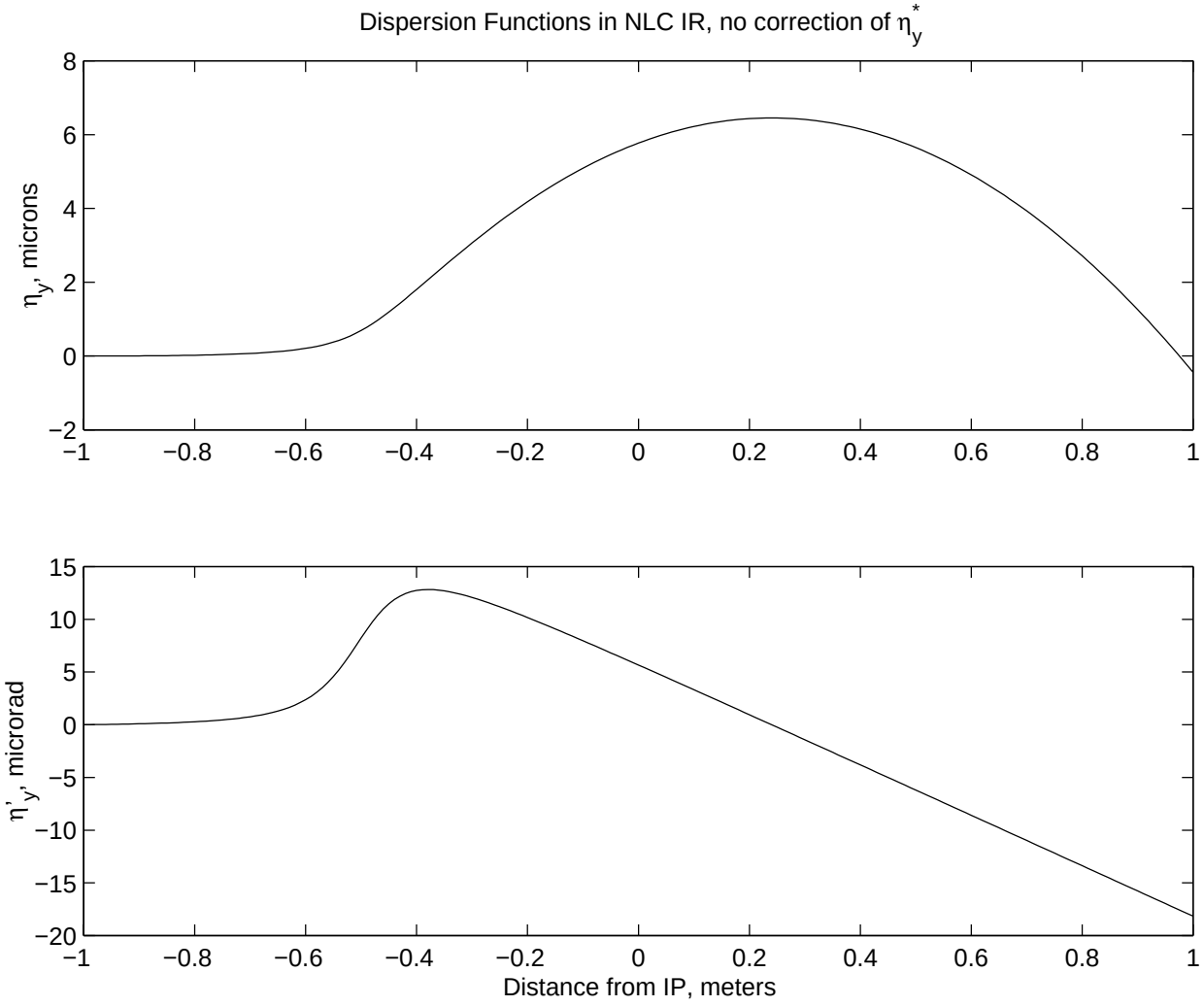

Figure 5: η_y and η'_y in the IR region, assuming no correction of η^*_y.

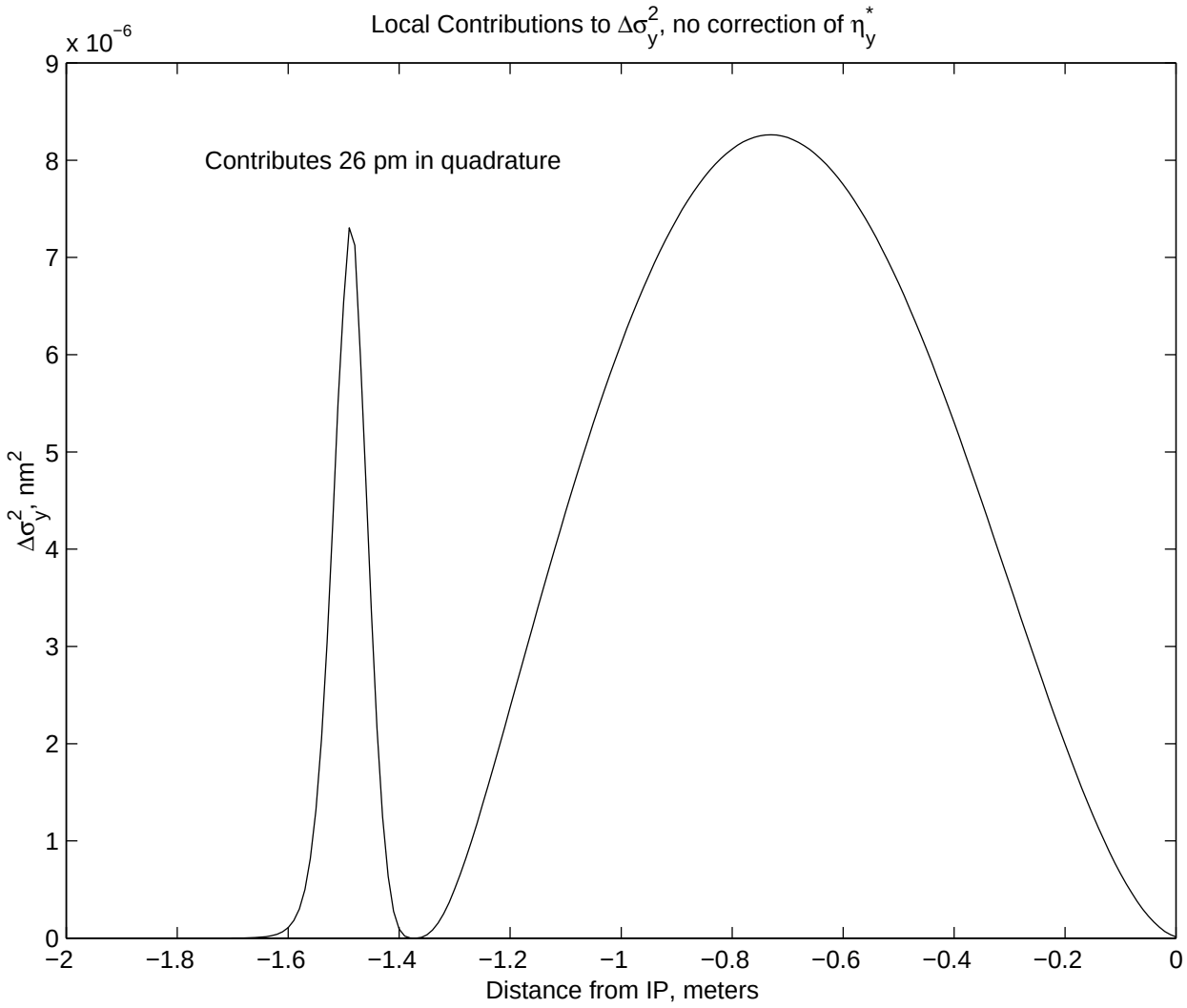

Figure 6: Local contributions to the IP beam size increase due to SR in the case where η_y^* is not corrected.

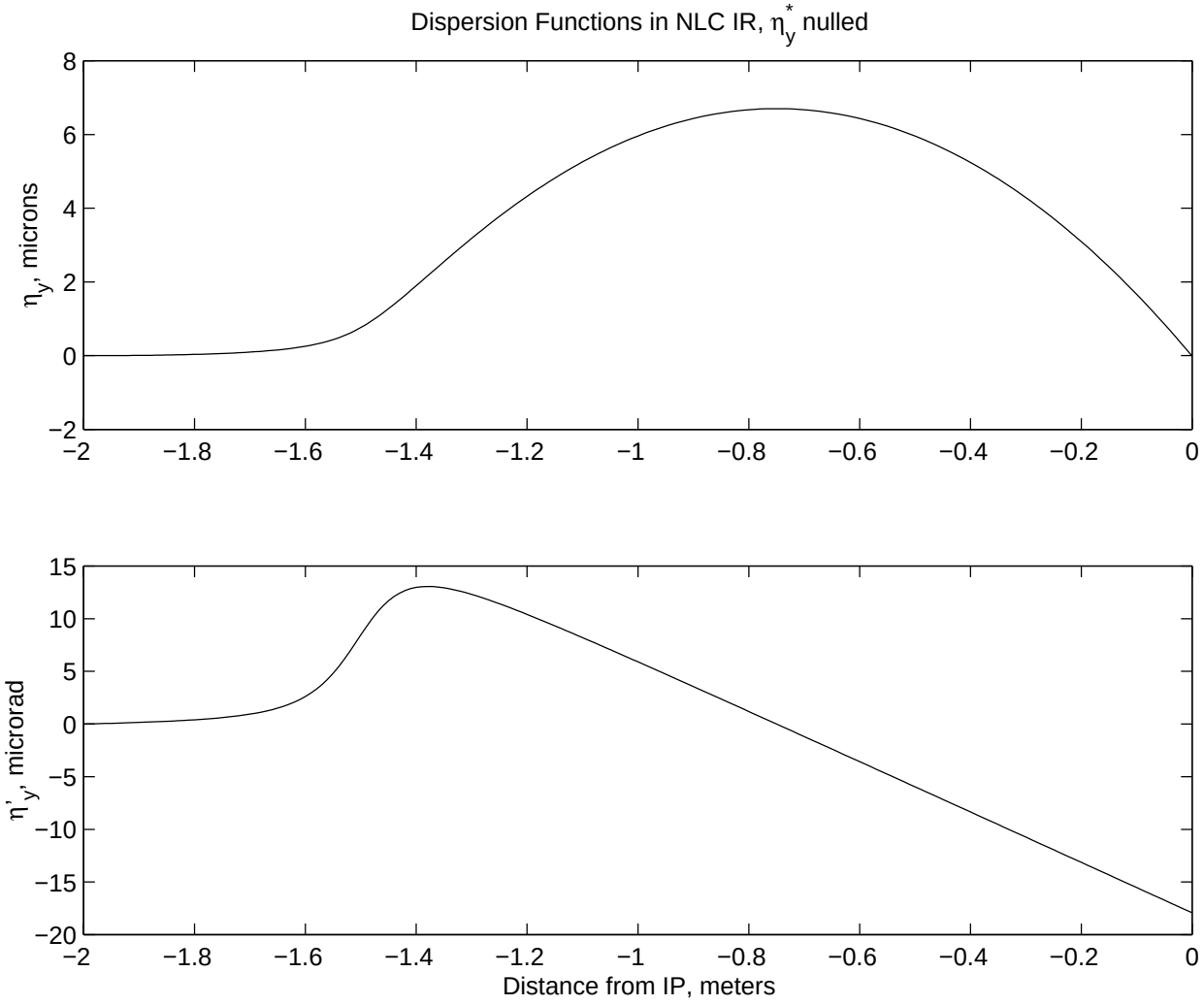

Figure 7: η_y and η'_y functions when a corrector is used to zero η^*_y.

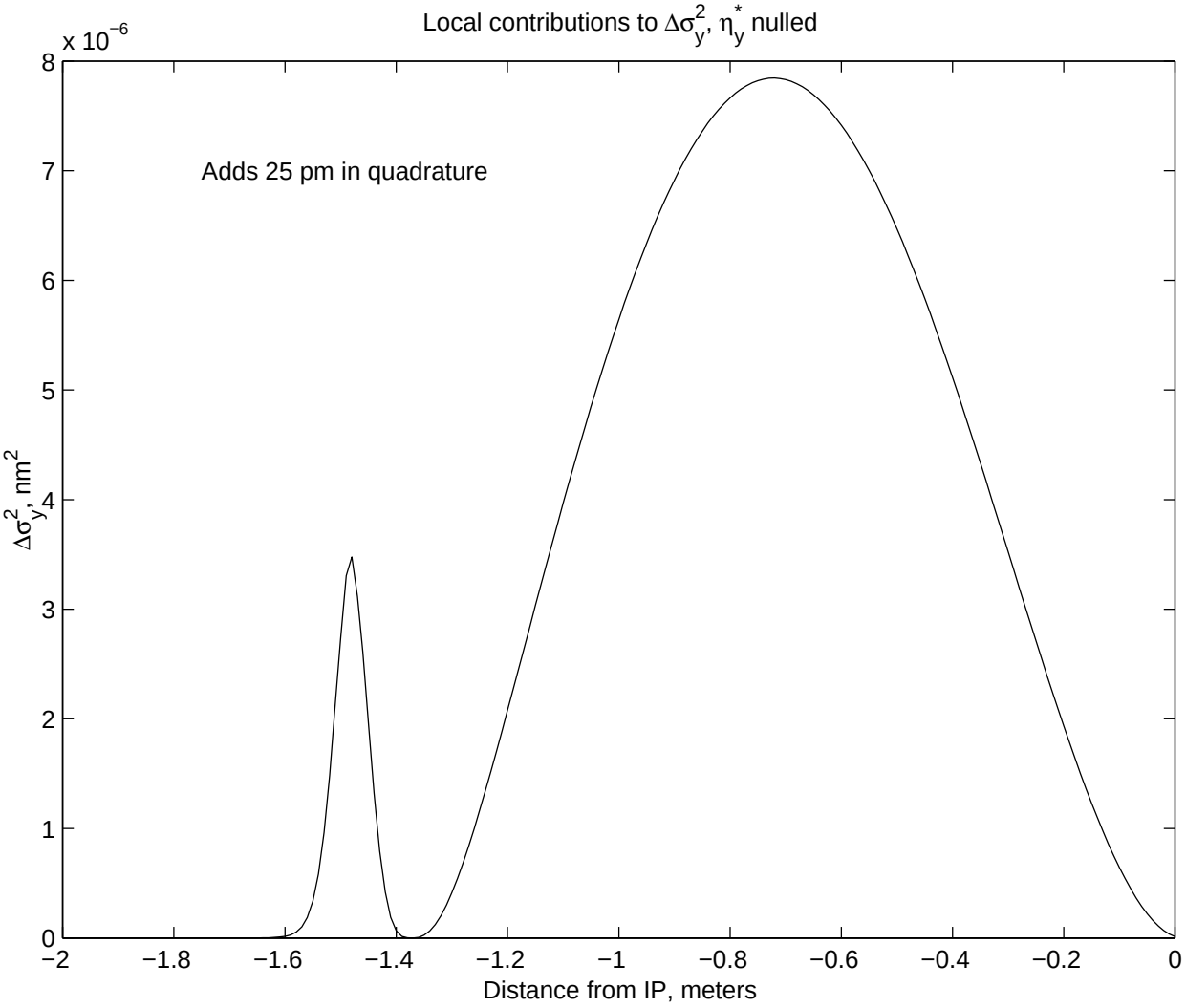

Figure 8: Local contributions to IP beam size increase due to SR in the case where η_y^* is nulled.